In Vivo Visualization of Endoplasmic Reticulum Stress in the Retina Using the ERAI Reporter Mouse

Marcel V. Alavi,[1] Wei-Chieh Chiang,[2] Heike Kroeger,[2] Douglas Yasumura,[*,1] Michael T. Matthes,[1] Takao Iwawaki,[3] Matthew M. LaVail,[1] Douglas B. Gould,[1,4] and Jonathan H. Lin[2,5]

[1]Department of Ophthalmology, University of California, San Francisco, San Francisco, California, United States
[2]Department of Pathology, University of California, San Diego, La Jolla, California, United States
[3]Advanced Scientific Research Leaders Development Unit, Gunma University, Gunma, Japan
[4]Department of Anatomy and Institute for Human Genetics, University of California, San Francisco, San Francisco, California, United States
[5]VA San Diego Healthcare System, San Diego, California, United States

Correspondence: Jonathan H. Lin, Department of Pathology, University of California, San Diego, La Jolla, CA, USA;
JLin@ucsd.edu.

*Deceased May 4, 2014.

MVA and W-CC contributed equally to the work presented here and should therefore be regarded as equivalent authors.

Submitted: March 26, 2015
Accepted: August 3, 2015

Citation: Alavi MV, Chiang W-C, Kroeger H, et al. In vivo visualization of endoplasmic reticulum stress in the retina using the ERAI reporter mouse. *Invest Ophthalmol Vis Sci*. 2015;56:6961–6970. DOI:10.1167/iovs.15-16969

Purpose. Endoplasmic reticulum (ER) stress activates inositol requiring enzyme 1 (IRE1), a key regulator of the unfolded protein response. The *ER stress activated indicator* (*ERAI*) transgenic mouse expresses a yellow fluorescent GFP variant (Venus) when IRE1 is activated by ER stress. We tested whether *ERAI* mice would allow for real-time longitudinal studies of ER stress in living mouse eyes.

Methods. We chemically and genetically induced ER stress, and qualitatively and quantitatively studied the Venus signal by fluorescence ophthalmoscopy. We determined retinal cell types that contribute to the signal by immunohistology, and we performed molecular and biochemical assays using whole retinal lysates to assess activity of the IRE1 pathway.

Results. We found qualitative increase in vivo in fluorescence signal at sites of intravitreal tunicamycin injection in *ERAI* eyes, and quantitative increase in *ERAI* mice mated to Rho^{P23H} mice expressing ER stress-inducing misfolded rhodopsin protein. As expected, we found that increased Venus signal arose primarily from photoreceptors in $Rho^{P23H/+}$*;ERAI* mice. We found increased $Xbp1^{S}$ and XBP1s transcriptional target mRNA levels in $Rho^{P23H/+}$*;ERAI* retinas compared to $Rho^{+/+}$*;ERAI* retinas, and that Venus signal increased in *ERAI* retinas as a function of age.

Conclusions. Fluorescence ophthalmoscopy of *ERAI* mice enables in vivo visualization of retinas undergoing ER stress. *ER stress activated indicator* mice enable identification of individual retinal cells undergoing ER stress by immunohistochemistry. *ER stress activated indicator* mice show higher Venus signal at older ages, likely arising from amplification of basal retinal ER stress levels by GFP's inherent stability.

Keywords: ER stress, GFP, funduscopy

The endoplasmic reticulum (ER) organelle is essential for folding of secretory and membrane proteins, lipid and sterol synthesis, and intracellular calcium storage.[1] Diverse environmental and pathologic insults, including protein misfolding, oxidative stress, hypoxia, infection, and inflammation, interfere with ER functions and cause ER stress.[2] Chronic ER stress triggers cell death, and has been implicated in the pathogenesis and progression of a wide variety of eye diseases, including age-related macular degeneration, glaucoma, and retinitis pigmentosa.[3–7] Transgenic mice expressing fluorescent proteins induced by ER stress[8] or protein misfolding[9,10] provide a means to track ER stress in real time in live animals at single cell resolution under normal or disease conditions. In principle, these in vivo reporters also could reveal temporal fluctuations in ER stress levels that are too dynamic to detect by in vitro approaches. Here, we qualitatively and quantitatively defined the ability of the *ER stress activation indicator* (*ERAI*) mouse, a transgenic line that produces green fluorescent protein (Venus) in response to ER stress, to report changes in ER stress levels in live rodent retina by funduscopic imaging accompanied by histologic, biochemical, and molecular analysis of postmortem retinal tissues.

ER stress activation indicator mice carry a *Xbp1-Venus* fusion transgene expressed under the control of CMV-β actin promoter that drives transgene expression in all tissues.[8] As illustrated in Figure 1A, the endogenous *Xbp1* mRNA contains a small intron that is specifically spliced by inositol-requiring enzyme 1 (IRE1) only when IRE1 has been activated by ER stress.[2] Spliced *Xbp1* mRNA subsequently produces a potent transcription factor XBP1s that upregulates ER protein folding chaperones and ER-associated protein degradation components to reduce misfolded protein levels and thereby alleviates ER stress.[11,12] In the *Xbp1-Venus* reporter, the inhibitory intron is retained so that fluorescent Venus protein is produced only when ER stress has activated the IRE1 protein (Fig. 1B).[8] Thus, the production of fluorescent signal in *ERAI* mice provides a highly specific readout for ER stress. Importantly, the transcrip-

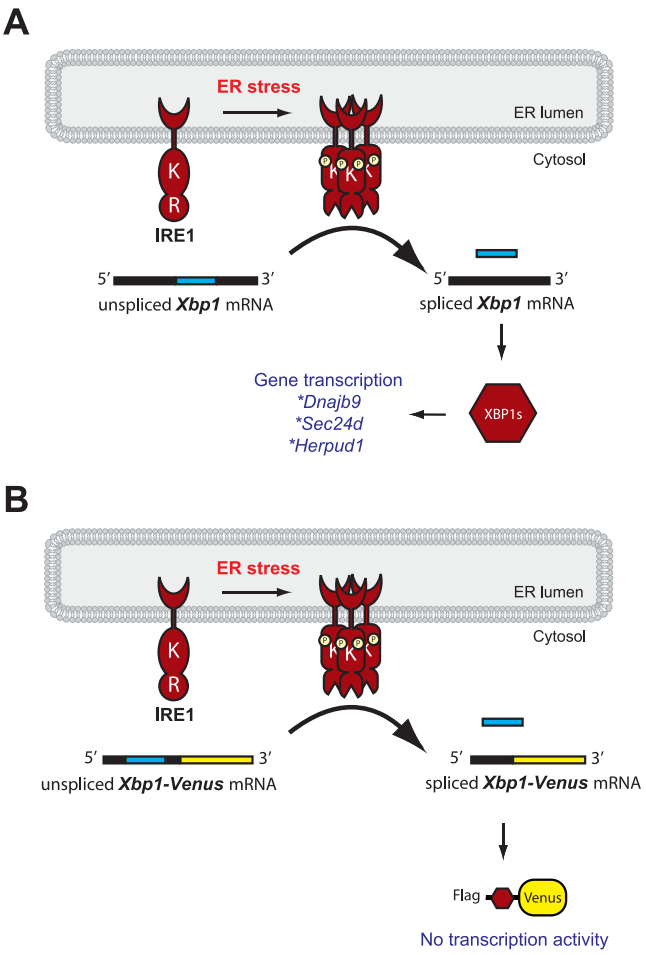

Figure 1. Schematic of the mammalian IRE1 pathway and the function of the XBP1-Venus reporter. Unfolded proteins in the ER (= ER stress) activate IRE1, which splices out an intron of the *Xbp1* mRNA. Spliced *Xbp1* encodes the transcription factor XBP1s, which upregulates proteins that alleviate ER stress (**A**). Upon activation, IRE1 also can remove an intron of an *Xbp1-Venus* reporter transgene in *ERAI* mice. Spliced *Xbp1-Venus* mRNA encodes a transcriptional inactive, cytosolic XBP1-Venus fusion protein, which allows for monitoring IRE1 activity by its fluorescence signal (**B**).

tional activator domain has been deleted from XBP1-Venus, and no adverse effects have been reported in these transgenic mice.

The *ERAI* mouse has proven useful in identifying retinal cells undergoing ER stress through confocal microscopy analysis of enucleated eyes and by fluorescence ophthalmoscopy of qualitative fluorescent signal.[13–15] Here, we quantitatively measured Venus fluorescence by imaging in *ERAI* mice exposed to chemical or genetic types of ER stress lasting up to nine months. In parallel, we performed quantitative biochemical and molecular measurements of endogenous *Xbp1* splicing and function over the same timespan. We found that ER stress increased Venus signal as well as endogenous $Xbp1^S$ production. Quantification revealed that the magnitude of XBP1-Venus was significantly greater compared to endogenous $Xbp1^S$ induction. Based on these findings, we proposed that *ERAI* mice are well suited for qualitative in vivo and in vitro identification of ocular structures and cell types undergoing ER stress. However, quantitative assessments of ocular ER stress levels using *ERAI* animals should take into account differences between Venus reporter signal and endogenous $Xbp1^S$ induction.

Methods

Animals

Transgenic *ERAI* mice[8] and Rho^{P23H} knock-in mice[16] have been described. *ER stress activation indicator* mice were on a C57BL/6JJcl and Rho^{P23H} knock-in mice on a C57BL/6J genetic background. We confirmed by DNA sequencing[17] that Rho^{P23H} mice do not carry the $Crb1^{rd8}$ allele, which causes recessively inherited retinal degeneration.[18] All data were obtained in hemizygous *ERAI* animals heterozygous for $Crb1^{rd8}$. The C57BL/6 genetic background suppresses the retinal degeneration phenotype associated with recessive *Crb1* mutations,[18] and we did not observe the intraretinal spots characteristic for this phenotype in heterozygous $Crb1^{rd8/+}$;*ERAI* mice (Supplementary Figs. S1A–J). Animals were kept in a 12-hour light/12-hour dark cycle in full-barrier facilities free of specific pathogens with food (standard rodent diet) and water available ad libitum. Mouse breeding, and all experimental studies and procedures were performed in accordance with the guidelines of the Institutional Animal Care and Use Committee at the University of California, San Francisco and in compliance with the ARVO Statement for the Use of Animals in Ophthalmic and Vision Research.

In Vivo Imaging

Mice were anesthetized by inhalation of a constant flow of 1.5% to 3.0% isoflurane, and eyes were dilated with one drop of 1% tropicamide and one drop of 2.5% phenylephrine. Corneas were kept moist with regular application of 2.5% methylcellulose. Both eyes of each animal were examined with a Micron III retinal imaging system (Phoenix Research Labs, Pleasanton, CA, USA). Color fundus images were acquired (single frame, medium light intensity) as RGB TIFF images. Fluorescence ophthalmoscopy was done on the same instrument using a BrightLine single-band filter set optimized for yellow fluorescent protein (YFP-2427B-000; Semrock, Lake Forest, IL, USA), and images were acquired with defined settings for light intensity, exposure time, and gain. We quantified fluorescence as the mean intensity of all pixels in the green channel of the unadjusted RGB TIFF images from the fundus camera using ImageJ 1.47m (http://imagej.nih.gov/ij/; provided in the public domain by the National Institutes of Health, Bethesda, MD, USA). For illustration of the fundus, the native TIFF images were adjusted with levels and sharpened (unsharp mask, 100%, 2 px) using Photoshop CS6 (Adobe, San Jose, CA, USA). Spectral-domain optical coherence tomography (OCT) images were acquired with the Micron Image Guided OCT System (Phoenix Research Labs) by averaging 10 scans, and levels were adjusted to optimize the tonal range of the images using Photoshop CS6 (Adobe).

Intravitreal Injections

Tunicamycin (0.5 μL 20 μg/mL; EMD Millipore, Billerica, MA, USA) or dimethyl sulfoxide (DMSO) was injected into the vitreous of *ERAI* mice ($n = 3$) at P120, and eyes were examined by funduscopy, in vivo fluorescence ophthalmoscopy, and OCT at indicated time points after injection.

Morphology, Immunohistochemistry, and Microscopy

Analysis of retinal morphology has been described previously.[15] For immunohistochemistry, eyes were enucleated and fixed by immersion in 4% paraformaldehyde in PBS for 1 hour at room temperature. After overnight incubation with 30% sucrose at 4°C, eyes were frozen in Optimal Cutting Temperature (O.C.T.)

compound (Tissue-Tek; Sakura Finetek, Torrance, CA, USA). Sections (8 μm) were cut through the optic nerve head and labeled with indicated antibodies. Sections were blocked with 5% goat serum in 1% BSA/PBS and 0.1% Triton X-100 for 1 hour, followed by incubation with a primary antibody at 4°C overnight. Primary antibodies used were 1D4 anti-rhodopsin antibody at 1:500 dilution (Santa Cruz Biotechnologies, Santa Cruz, CA, USA) and anti-GFP at 1:250 (Invitrogen, Carlsbad, CA, USA). After washing in 0.1% Triton X-100 in PBS three times, sections were incubated with secondary antibodies that included Alexa 546 goat anti-mouse (red) antibody (Molecular Probes, Eugene, OR, USA; Invitrogen) and Alexa 488 goat anti-rabbit (green) antibody (Molecular Probes) used at a dilution of 1:500. After washing in PBS three times, cover slips were mounted in ProLong Gold antifade reagent with 4′,6-diamidino-2-phenylendole (DAPI; Invitrogen), and images were collected with an Olympus FluoView-1000 confocal microscope and processed using Olympus FluoView Ver.2.0a Viewer software (Olympus Corporation, Tokyo, Japan) at the University of California, San Diego (UCSD) microscopy facility.

Quantitative PCR

Total retinal RNA was collected with an RNeasy mini kit (Qiagen, Hilden, Germany). mRNA was reverse-transcribed with the iScript cDNA Synthesis Kit (Bio-Rad Laboratories, Inc., Hercules, CA, USA). For quantitative PCR (qPCR) analyses, cDNA were used as templates in SYBR green qPCR supermix (Bio-Rad Laboratories, Inc.). Primers included: *Ddit3*, 5′-ACGGAAACAGAGTGGTCAGTGC-3′ and 5′-CAGGAGGT GATGCCCACTGTTC-3′; *Dnajb9*, 5′-TAAAAGCCCTGATGCT GAAGC-3′ and 5′-TCCGACTATTGGCATCCGA-3′; *Herpud1*, 5′-ACCGCAGTTGGAGTGTGAGTCG-3′ and 5′-TCTGGCATTTTG GAGGGATTCTTC-3′; *Hspa5*, 5′-CCTGCGTCGGTGTGTTCAAG-3′ and 5′-AAGGGTCATTCCAAGTGCG-3′; *Rpl19*: 5′-ATGC CAACTCCCGTCAGCAG-3′ and 5′-TCATCCTTCTCATCCAGGT CACC-3′; *Sec24d*, 5′-TCTTTGCCTACTGCCGAAGCAC-3′ and 5′-GACCCAAGGAAGCCACATCCAC-3′; $Xbp1^S$, 5′-GAGTCCGCAG CAGGTG-3′ and 5′-GTGTCAGAGTCCATGGGA-3′. For all qPCR analysis, *Rpl19* mRNA levels, a transcript with levels unaltered by ER stress, served as internal normalization standards. Quantitative PCR conditions were 95°C for 5 minutes, 95°C for 10 seconds, 60°C for 10 seconds, 72°C for 10 seconds, with 50 cycles of amplification.

Statistical Analysis

Fluorescence intensities at P120 from at least 8 eyes of wild-type mice, $Rho^{+/+}$ mice, and $Rho^{P23H/+}$ mice were compared by a 1-way ANOVA (PRISM; GraphPad Software, Inc., La Jolla, CA, USA) and presented as scatter plot showing the means ± SD. Fluorescence intensities at different ages were plotted as means ± SD for the indicated sample size of $Rho^{+/+}$ mice and $Rho^{P23H/+}$ mice, and a linear regression or nonlinear regression model ($f = a^*[1 - \exp(-b^*x)]$) was calculated for $Rho^{+/+}$ mice and $Rho^{P23H/+}$ mice, respectively (SigmaPlot 12; Systat Software, Inc., San Jose, CA, USA). For qPCR data, results are presented as means ± SD from at least five mice per experimental condition. All data (unless stated otherwise) were compared by Student's 2-tailed *t*-tests and differences were considered statistically significant for P values below 0.05 and highly significant for $P < 0.001$.

Results

We tested whether we could monitor ER stress in vivo with *ERAI* mice. For this, we injected tunicamycin, an agent that strongly induces ER stress by inhibiting N-linked protein glycosylation,[19,20] intravitreally into the superior hemisphere of one eye of hemizygous *ERAI* mice. The second eye was injected with DMSO as vehicle control (Fig. 2). Two days after injection, funduscopy revealed areas of bright lesions in the superior hemisphere of the tunicamycin-injected eyes (Fig. 2D), which correlated with attenuation of the well-defined layering of the photoreceptor outer segments and RPE as viewed by OCT (Fig. 2E; compare to DMSO-injected wild-type OCT in Fig. 2B, asterisk). The superior, tunicamycin-injected hemisphere showed increased fundus fluorescence compared to the inferior part of the eye (Fig. 2F) and the contralateral control eye that received DMSO (Fig. 2C). At 7 days post injection, the retina of the tunicamycin-injected eye showed advanced disruption and widespread fluorescence (Figs. 2G–I). By 27 days post injection, the superior region of the tunicamycin-injected eye showed degeneration of the outer retinal layers (Fig. 2K) and decreased fluorescence in the superior hemisphere (Fig. 2L). Still, the remaining areas in the tunicamycin-injected eye showed augmented fluorescence, which further increased over time until the animals were killed 70 days after injection. These results demonstrate that ophthalmic examination is capable of monitoring qualitative changes in chemically-induced ER stress in *ERAI* mice in vivo.

Next, we tested the specificity and sensitivity of *ERAI* in monitoring genetic causes of ER stress in vivo. We crossed *ERAI* mice with the Rho^{P23H} knock-in mouse line carrying the p.P23H rhodopsin mutation,[16] which is the most common mutation in patients with autosomal dominant retinitis pigmentosa in the United States.[21,22] The P23H mutation causes rhodopsin protein misfolding and induces ER stress in heterologous cell culture systems and in rodent models of retinal degeneration.[15,23–26] Heterozygous $Rho^{P23H/+}$ mice show progressive photoreceptor loss as they age,[16] and by P120, the ONL thickness is only 50% compared to wild-type $Rho^{+/+}$ mice (see Fig. 6A). We compared $Rho^{+/+}$ wild-type mice without the *ERAI* transgene (Figs. 3A–C) to $Rho^{+/+}$;*ERAI* animals (Figs. 3D–F) and $Rho^{P23H/+}$;*ERAI* animals (Figs. 3G, 3H) of the same genetic background. Funduscopy of all three lines at P120 appeared unremarkable (Figs. 3A, 3D, 3G). Morphologic analysis of two P120 $Rho^{+/+}$;*ERAI* retinas was without pathologic findings (Supplementary Figs. S1K, S1L) and OCT further confirmed the retinal integrity in the analyzed mice (Fig. 3F). $Rho^{P23H/+}$;*ERAI* mice showed advanced photoreceptor loss and shortening of the outer segments by OCT (compare Figs. 3E, 3H). We measured the fluorescence signal coming from the Venus protein as read-out for ER stress by funduscopic imaging. Wild-type mice did not show any detectable fluorescence signal (Figs. 3C, 3I), while *ERAI* mice of both genotypes showed clearly detectable fluorescence (illustrated in Fig. 3F). When we quantified the fluorescence, we found a significantly stronger Venus signal in $Rho^{P23H/+}$;*ERAI* mice compared to $Rho^{+/+}$;*ERAI* animals ($P < 0.001$; $Rho^{P23H/+}$, $n = 15$; $Rho^{+/+}$, $n = 11$; Fig. 3I). These results demonstrated that funduscopic ophthalmic examination of *ERAI* mice enables monitoring of changes in genetic forms of ER stress in vivo.

Next, we investigated temporal changes in Venus fluorescence signal from retinas in $Rho^{+/+}$;*ERAI* and $Rho^{P23H/+}$;*ERAI* mice. To this end, we examined animals in vivo by OCT and fluorescence funduscopy from 1 to 9 months of age. The fundus was unremarkable (Supplementary Fig. S1) and OCT revealed no retinal deterioration in $Rho^{+/+}$;*ERAI* mice (Figs. 4A–E). We found progressive thinning of the outer retina in $Rho^{P23H/+}$;*ERAI* mice by OCT (Figs. 4F–J). When we examined the same retinas for Venus signal by fluorescence ophthalmoscopy, we found an age-related increase in the fluorescence signal in $Rho^{P23H/+}$;*ERAI* animals (Figs. 4P–T). Interestingly, we

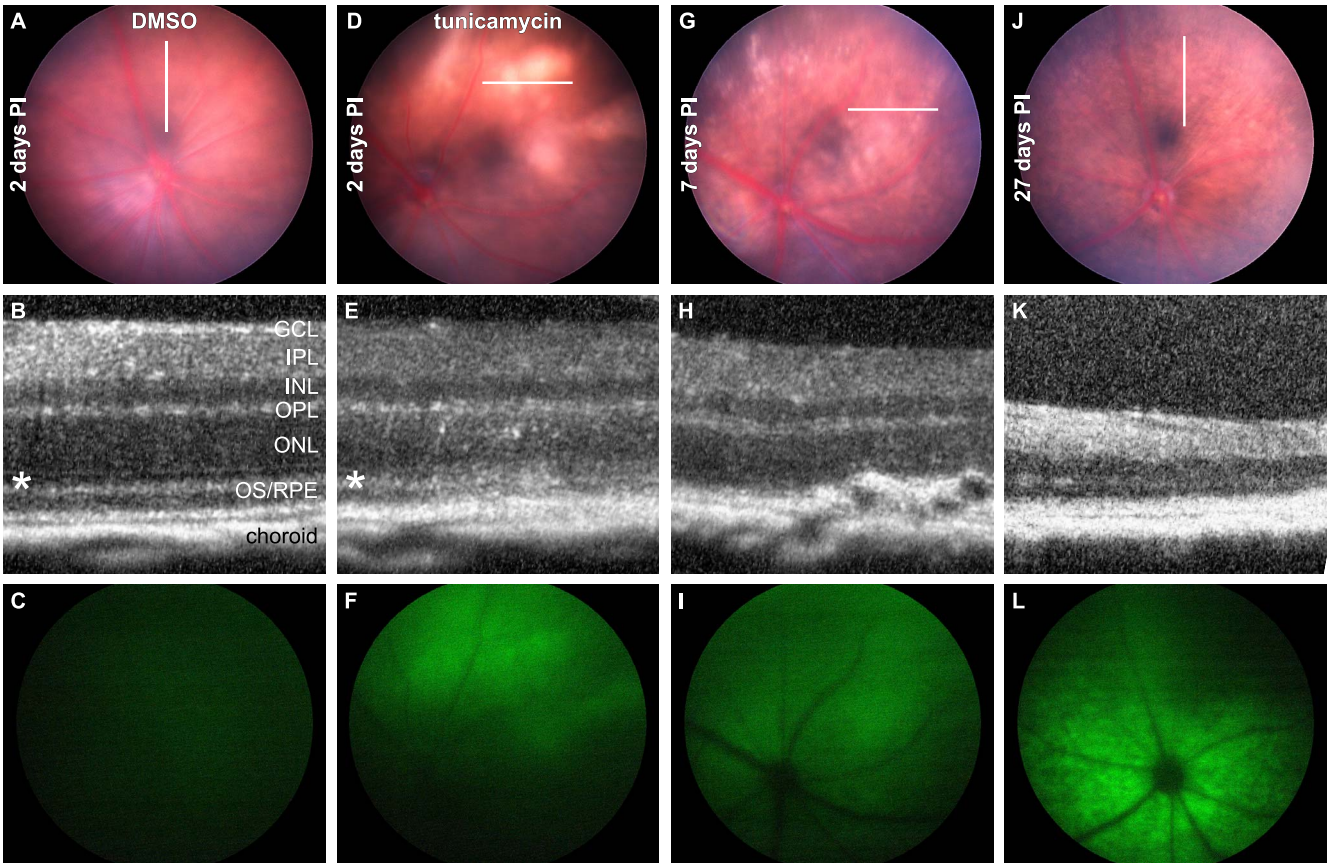

Figure 2. In vivo monitoring IRE1 activation upon tunicamycin injections in ERAI mice. Dimethyl sulfoxide–injected eyes showed no pathologic findings after 2 days (**A–C**), while tunicamycin-injected eyes showed disbanding of the photoreceptor segments (*asterisk* in [**E**]) and increased fluorescence at the injection site ([**F**], *superior hemisphere*). With progressing degeneration fluorescence signals extended beyond the superior hemisphere (**G–I**) until most of the outer retinal layers were missing and the superior hemisphere showed little or no fluorescence anymore (**K–L**). PI, post injection; GCL, ganglion cell layer; IPL, inner plexiform layer; INL, inner nuclear layer; OPL, outer plexiform layer; ONL, outer nuclear layer; OS/RPE, outer segments–RPE complex.

also saw a progressive increase in Venus signal in *Rho*$^{+/+}$*;ERAI* mice over the same time frame (Figs. 4K–O). These findings indicated that Venus signal in *Rho*$^{P23H/+}$*;ERAI* and *Rho*$^{+/+}$*;ERAI* mice increased with age.

To determine which retinal cell type(s) generated the Venus signal, we performed confocal microscopy on immunolabeled histologic sections of eyes from *Rho*$^{+/+}$*;ERAI* mice and *Rho*$^{P23H/+}$*;ERAI* mice (Fig. 5). The strongest labeling against Venus protein in *Rho*$^{P23H/+}$*;ERAI* mice was found in photoreceptors (Fig. 5C), consistent with prior studies.[14,15] Interestingly, photoreceptors also were the predominant Venus-expressing retinal cell type in *Rho*$^{+/+}$*;ERAI* mice even though they did not express mutant protein (Fig. 5B). Of note, occasional cells in the ganglion cell and inner nuclear layers also showed Venus staining in *Rho*$^{+/+}$*;ERAI* mice and *Rho*$^{P23H/+}$*;ERAI* mice. Venus is a cytosolic protein,[8] and the labeling in *Rho*$^{+/+}$*;ERAI* mice was most prominent in the photoreceptor inner segments and was excluded from the outer segments (Figs. 5A, 5B). When we compared Venus signal from eyes of *Rho*$^{+/+}$*;ERAI* mice at P30 (Fig. 5A), we saw significantly less Venus labeling compared to the older animals at P120 (Fig. 5B), consistent with our in vivo imaging results. To rule out that the increased signal in P120 *Rho*$^{+/+}$*;ERAI* mice compared to P30 *Rho*$^{+/+}$*;ERAI* mice related to funduscopic or confocal imaging artifacts, we performed Western blot analyses against the Venus protein and the Flag-tag at the amino-terminus of the *ERAI* reporter construct[8] using whole retinal lysates collected from P5 to P270 (Fig. 6B). We found that Venus and FLAG protein levels were significantly higher in older mice. Taken together, the histologic findings revealed that photoreceptors were the predominant retinal cell type expressing Venus. Moreover our histologic and biochemical analysis further supported the age-related increase in Venus signal that we have discovered in vivo by fluorescence ophthalmoscopy.

Next, we examined quantitative differences in Venus fluorescence between *Rho*$^{+/+}$*;ERAI* mice and *Rho*$^{P23/+}$*;ERAI* mice over time. At P30, we found significant and quantitatively stronger fluorescence in eyes of *Rho*$^{P23H/+}$*;ERAI* mice ($n = 9$) compared to those in *Rho*$^{+/+}$*;ERAI* mice ($n = 10$, $P = 0.037$; Fig. 6C). At P60 (*Rho*$^{P23H/+}$, $n = 8$; *Rho*$^{+/+}$, $n = 4$), P90 (*Rho*$^{P23H/+}$, $n = 16$; *Rho*$^{+/+}$, $n = 13$), and P120 (*Rho*$^{P23H/+}$, $n = 15$; *Rho*$^{+/+}$, $n = 11$), we found highly significantly increased Venus fluorescence signal in eyes of *Rho*$^{P23H/+}$*;ERAI* animals ($P < 0.001$ for all time points; Fig. 6C). However, at P270, we found no significant difference in the fluorescence signal compared to *Rho*$^{+/+}$*;ERAI* mice ($n = 6$ for both genotypes, $P = 0.476$; Fig. 6C). Our histologic studies identified photoreceptors as the predominant retinal cell type expressing Venus (Fig. 5), and photoreceptors are lost in *Rho*$^{P23H/+}$*;ERAI* mice as they age (Figs. 4, 6A). Therefore, increases in Venus fluorescence in *Rho*$^{P23H/+}$*;ERAI* mice as they aged were likely offset by concomitant loss of the photoreceptors expressing the Venus protein. Indeed, when we normalized our quantification of Venus fluorescence signal to ONL thickness (as a proxy for the number of photoreceptors remaining), we identified substan-

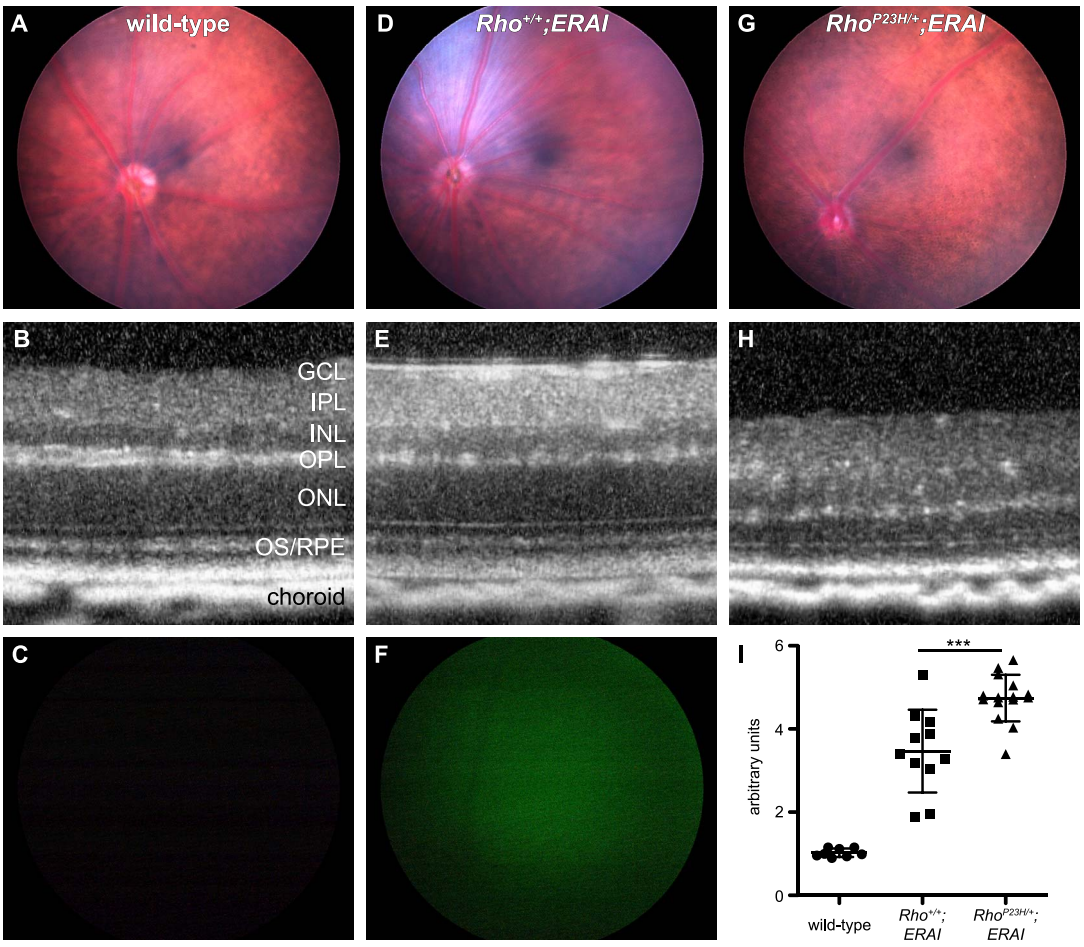

Figure 3. In vivo assessment of genetically-induced ER stress in retinas of *Rho*$^{P23H/+}$*;ERAI* mice. Misfolded rhodopsin causes ER stress and progressive photoreceptor degeneration. Nontransgenic wild-type mice (**A–C**) did not show any detectable fundus fluorescence in the Venus wavelength range, while *Rho*$^{+/+}$*;ERAI* mice (**D–F**) and *Rho*$^{P23H/+}$*;ERAI* mice (**G–H**) showed clearly detectable Venus fluorescence signals, which were highly significantly stronger in *Rho*$^{P23H/+}$*;ERAI* mice (**I**). ***$P < 0.001$.

tially more Venus signal in *Rho*$^{P23H/+}$*;ERAI* mice at all ages compared to *Rho*$^{+/+}$*;ERAI* mice (Fig. 6D).

Last, we examined whether endogenous *Xbp1* splicing and transcriptional function also showed the same increase that we observed with the Venus signal (itself produced by processing of the *Xbp1-Venus* transgene). For this, we performed molecular assays to quantify endogenous spliced *Xbp1* mRNA and mRNA levels of multiple downstream genes directly transcribed by the XBP1s protein. In *Rho*$^{+/+}$ mice, *Xbp1*^{S} levels at P60, P90, and P120 appeared to be elevated and relatively stable in these animals compared to P30 (Fig. 7A, white bars and dotted line). By contrast, in retinas of *Rho*$^{P23H/+}$ mice, *Xbp1*^{S} levels were significantly elevated compared to *Rho*$^{+/+}$ mice at ages P30 ($P = 0.018$) and P60 ($P = 0.016$), while at P90 there was only a trend ($P = 0.070$), and at P120 there was no longer a significant difference between the two genotypes ($P = 0.499$; Fig. 7A, black bars and solid line). Next, we measured mRNA levels of *Sec24d*, *Dnajb9*, *Herpud1*, and *Hspa5*, downstream transcriptional targets of XBP1s.[11,12] In *Rho*$^{+/+}$ mice, we found small, but significant increases in mRNA levels for all these XBP1s target genes in older mice compared to P30. For *Hspa5* mRNA levels significantly increased between P30 and P60 ($P = 0.023$; Fig. 6B) with no further changes detected at later time points. Both *Dnajb9* and *Herpud1* showed no significant difference between P30 and P60. However, we found a significant increase between P30 and P90 ($P = 0.045$ and $P = 0.041$, respectively; Fig. 6B), while *Sec24d* showed only a trend between these two ages ($P = 0.055$; Fig. 6B). At P120, *Sec24d* showed a significant upregulation compared to P30 ($P < 0.003$; Fig. 6B). For the *Rho*$^{+/+}$ mice, the increase in *Dnajb9* and *Herpud1* mRNA levels from P30 to P120 also correlated with the increase in the Venus fluorescence signal (Pearson Product Moment Correlation, $P < 0.05$). In summary, our molecular analysis of the *Rho*$^{+/+}$ mice showed relatively stable endogenous *Xbp1*^{S} mRNA levels accompanied by a mild increase in mRNA levels of downstream target genes in older mice. These findings raise the question of why does Venus signal increase so much more compared to levels of endogenous spliced *Xbp1* or its downstream target genes in the *Rho*$^{+/+}$ mice? We considered several possible sources for amplification of the Venus signal in the *Rho*$^{+/+}$ mice in the Discussion.

For the *Rho*$^{P23H/+}$ mice, *Sec24d*, *Dnajb9*, *Herpud1*, and *Hspa5* mRNA levels were significantly increased compared to levels in age-matched *Rho*$^{+/+}$ mice at all time points analyzed (*Sec24d*, $P = 0.002$; *Dnajb9* and *Herpud1*, $P < 0.001$; *Hspa5*, $P = 0.008$; Fig. 7C), consistent with the increase in *Xbp1s* found by qPCR in *Rho*$^{P23H/+}$ mice (Fig. 7A). In *Rho*$^{P23H/+}$ mice, *Sec24d* and *Hspa5* levels trended higher over time with no significant differences between any two time points (Fig. 7C). For *Dnajb9* and *Herpud1*, we found a significant difference between P30 and P60 ($P = 0.009$ and $P = 0.045$, respectively;

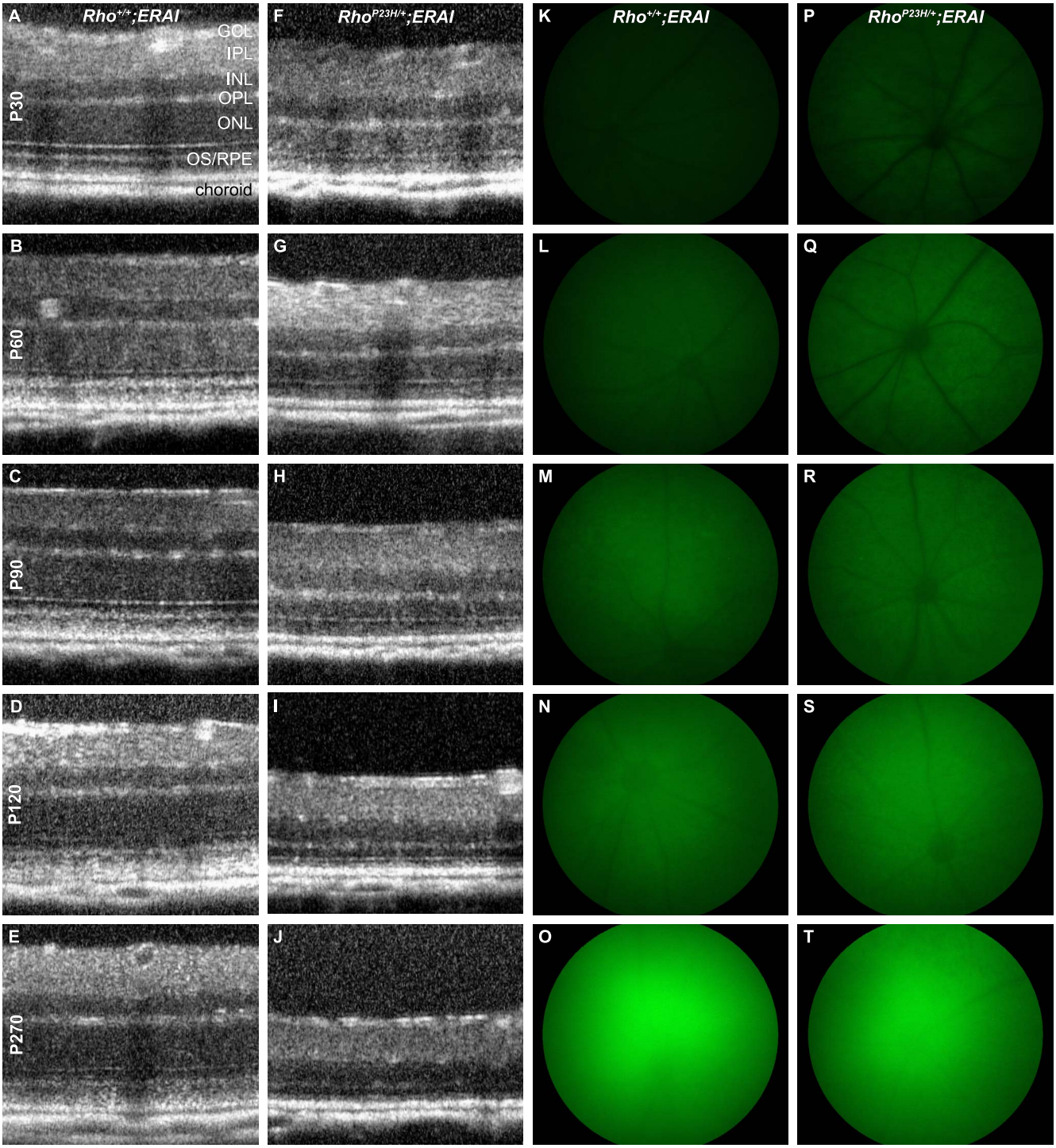

Figure 4. Age-dependent increase in fluorescence in *Rho*$^{+/+}$*;ERAI* mice and *Rho*$^{P23H/+}$*;ERAI* mice. Compared to *Rho*$^{+/+}$*;ERAI* mice (**A–E**), we found progressive photoreceptor degeneration in *Rho*$^{P23H/+}$*;ERAI* mice (**F–J**). Fluorescence ophthalmoscopy revealed age-dependent increase in Venus fluorescence in *Rho*$^{+/+}$*;ERAI* (**K–O**) and *Rho*$^{P23H/+}$*;ERAI* (**P–T**) mouse eyes, which appeared stronger in *Rho*$^{P23H/+}$*;ERAI* than in *Rho*$^{+/+}$*;ERAI* eyes at younger ages.

Fig. 7C), but not at subsequent time points. In summary, our molecular analysis of *Rho*$^{P23H/+}$ mice showed increased levels of XBP1s and downstream target genes at all ages compared to *Rho*$^{+/+}$ mice.

As a control, mRNA levels of *Ddit3/Chop*, another ER stress-induced gene regulated by the PERK pathway,[27] showed no changes over time or between genotypes in retinas of *Rho*$^{+/+}$ mice (Fig. 7B) and *Rho*$^{P23H/+}$ mice (Fig. 7C). This finding suggested that the increases we observed in mRNA levels of XBP1s target genes in *Rho*$^{+/+}$ and *Rho*$^{P23H/+}$ mice do not arise through a universal increase in gene expression or unified protein response (UPR) signaling activity as retinas age.

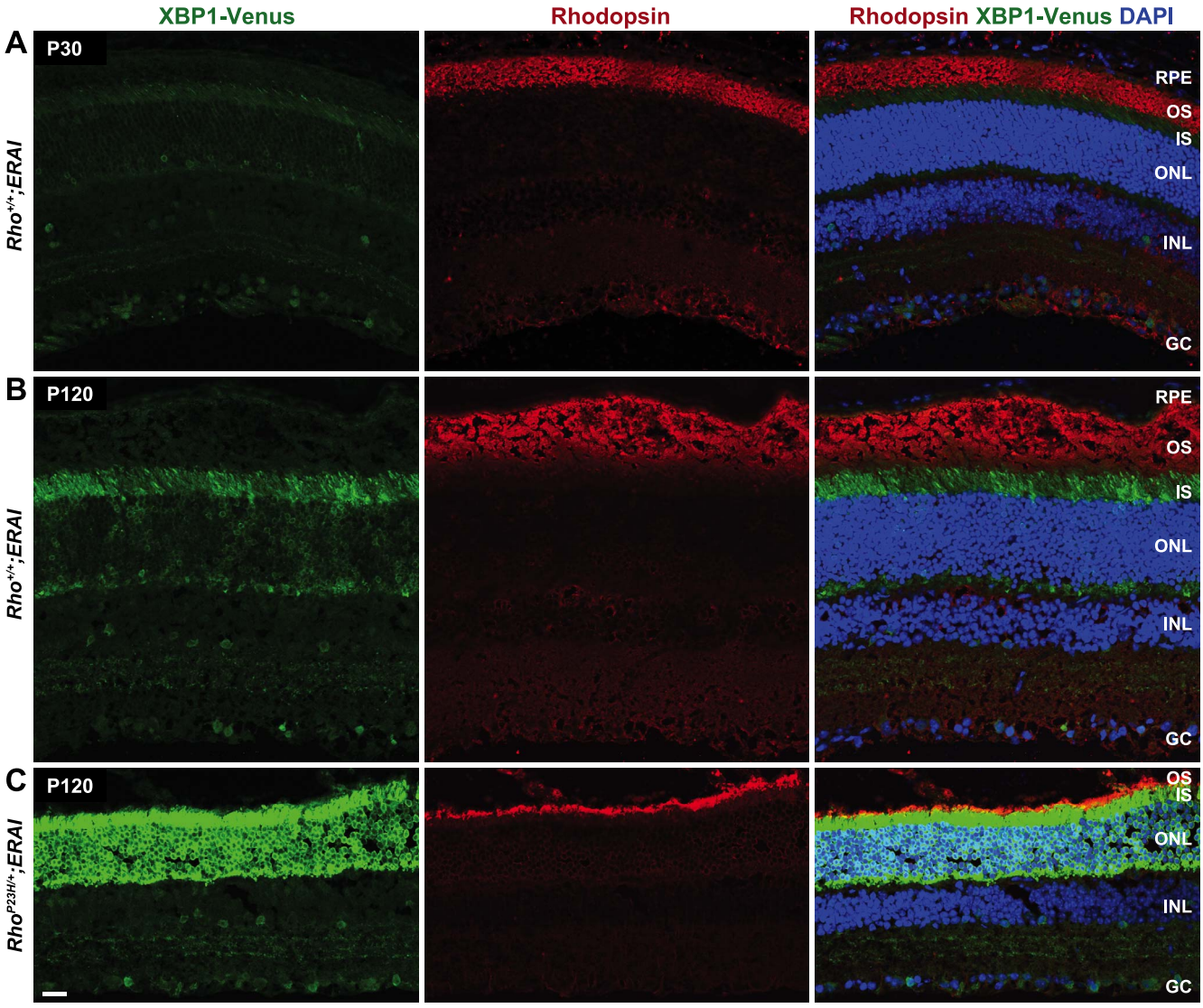

Figure 5. Immunohistochemistry against Venus and rhodopsin in *Rho*$^{+/+}$*;ERAI* and *Rho*$^{P23H/+}$*;ERAI* mice. *Rho*$^{+/+}$*;ERAI* eyes (**A**, **B**) and *Rho*$^{P23H/+}$*;ERAI* eyes (**C**) showed Venus labeling mainly in the photoreceptor layers, as well as single cells in the INL and GCL. Note the increased Venus labeling from P30 to P120 in *Rho*$^{+/+}$*;ERAI* mice (**A**, **B**). Rhodopsin (*red*), Venus (by anti-GFP, *green*), nuclear stain (DAPI, *blue*). *Scale bar*: 20 μm.

Discussion

Many transgenic reporter mice have been created that produce GFP in response to specific molecular stresses, including ER stress,[8] oxidative stress,[9,28] and protein misfolding.[9] In these reporter mice, the induction of GFP signal reveals which pathologic and environmental circumstances are associated with a molecular stress, at which point in a disease process this stress emerges, and fluorescently marks the tissues and cell types undergoing the stress. In the eye, the *ERAI* reporter mouse and a GFP protein misfolding reporter transgenic mouse have identified genetic mutations that trigger ER stress or protein misfolding problems in specific retinal cell types primarily through postmortem enucleation and histologic analysis of retinas from reporter mice crossed with mouse models of retinal disease.[10,13–15] Fluorescence ophthalmoscopy can detect GFP signal in living mouse eyes.[29] In stress-induced GFP reporter mice, fluorescence ophthalmoscopy could provide a way to track rapid and dynamic fluxes in ocular stress levels in the same live mouse over time that would not be possible by postmortem enucleation approaches. In this study, we qualitatively and quantitatively measured GFP fluorescence in *ERAI* mice undergoing chemical and genetic forms of ER stress conditions lasting up to 9 months. We compared changes in ER stress-induced fluorescence levels with changes in ER stress-induced splicing and gene transcription to determine how in vivo fluorescence ophthalmoscopy detection of ER stress correlates with conventional molecular assays used to detect ER stress.

Here, we found in vivo higher ocular signals by fluorescent ophthalmoscopy in *ERAI* mice challenged with chemical or genetic forms of ER stress. In parallel, we found increased mRNA levels of ER stress-induced genes by qPCR of whole retina lysates collected from *Rho*$^{P23H/+}$ mice. We also performed confocal microscopy on enucleated eyes from *Rho*$^{P23H/+}$*;ERAI* mice and found that fluorescent signal was predominantly confined to photoreceptors, the expected retinal cell type undergoing ER stress in *Rho*$^{P23H/+}$ mice. Together, our findings demonstrated that increased fluorescent signal corresponds to increased ER stress in *ERAI* mice. Based

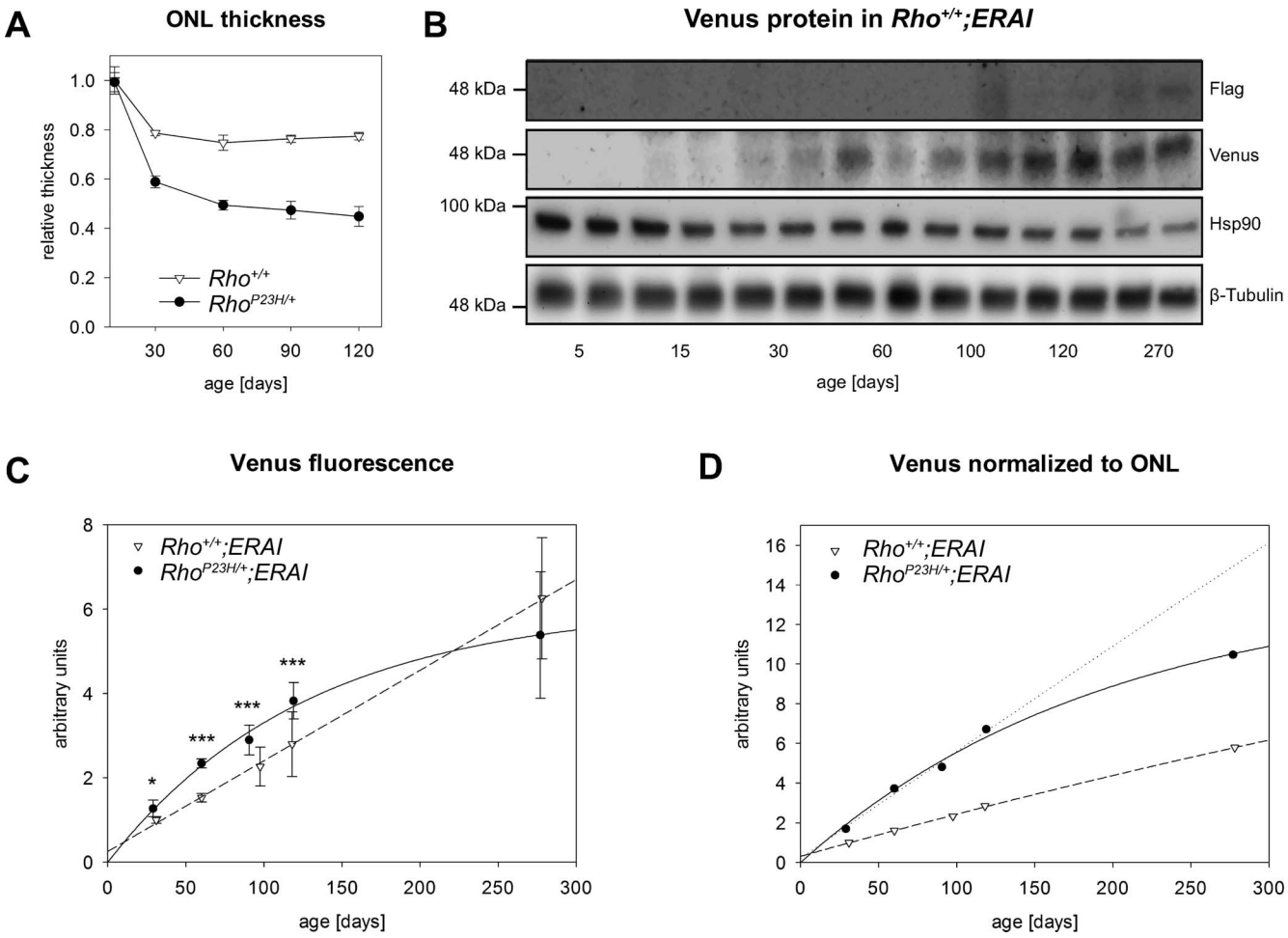

Figure 6. Evaluation of photoreceptor loss and Venus signals in *Rho*$^{+/+}$*;ERAI* and *Rho*$^{P23H/+}$*;ERAI* mouse retinas. Progressive photoreceptor loss in *Rho*$^{P23H/+}$ retinas compared to *Rho*$^{+/+}$ retinas (**A**). Western blot analysis revealed age-dependent increased antibody labeling against Venus and the amino-terminal Flag tag of the *ERAI* construct compared to Hsp90 and β-tubulin in *Rho*$^{+/+}$*;ERAI* retinas (**B**). Fundus fluorescence quantification at different ages showed linearly increased Venus in *Rho*$^{+/+}$*;ERAI* mice, while in P270 *Rho*$^{P23H/+}$*;ERAI* mice fluorescence leveled off (**C**). The Venus signal at younger ages was significantly higher in *Rho*$^{P23H/+}$*;ERAI* mice than in *Rho*$^{+/+}$*;ERAI* mice (**C**). Taking ONL thickness into account (shown in [**A**]), the relative fluorescence signals in *Rho*$^{P23H/+}$*;ERAI* mice vastly surpassed signals in *Rho*$^{+/+}$*;ERAI* mice at all ages (**D**). $^{*}P < 0.05$, $^{***}P < 0.001$.

on our experience, we propose that *ERAI* mice can be used reliably for in vivo identification of conditions that induce ER stress in the eye, although we cannot exclude functional electroretinographic deficits arising in the heterozygous *Crb1*$^{rd8/+}$ background, despite histologically normal retinal anatomy in these mice. Histochemical tissue analysis can subsequently identify the precise ocular cell type producing the signal, and with technologic advancements, in the near future, superresolution ophthalmoscopy may do this in vivo. Also as more genetically engineered animals carrying fluorescence reporter become available, standardized quantification of fluorescence signals across different imaging devices and platforms becomes an important issue. Delori et al.[30] resolved this problem by incorporating a small fluorescent plastic piece into the light path of the imaging device serving as internal fluorescent reference.

Quantification of fluorescent signal from *ERAI* mice in the absence of chemical or genetic sources of ER stress also showed a significant increase in fluorescence as these mice got older. What factors account for the increased fluorescence seen in aging *ERAI* mice? In lower organisms, ER stress levels increase as a function of age due to a decline in the fidelity of cellular protein quality control and protein homeostasis regulatory mechanisms concomitant with a build-up of misfolded proteins.[31,32] Age-related increase in retinal ER stress could be one factor contributing to the production of more fluorescent protein and signal seen in the *ERAI* mice. Indeed, we saw a mild increase in levels of ER stress-induced genes at P120 compared to P30 mouse retinas, but quantification revealed that the magnitude of increase in these molecular ER stress markers was much lower than the magnitude of fluorescence signal increase detected by ophthalmoscopy during the same period. A second factor that likely contributes to the larger increase in fluorescence signal relative to the increase observed in levels of molecular markers of ER stress is the inherent stability of fluorescent proteins. For example, the protein half-life of GFP—of which Venus is a variant[33]—is approximately 26 hours,[34] while the half-life of ER stress-induced proteins typically is less than an hour.[12] For example, the half-life of the XBP1s transcriptional activator is only 22 minutes.[35] The pronounced stability of the XBP1-Venus fusion protein magnifies small increases in ER stress and facilitates sensitive identification of retinal cells afflicted with ER stress in the *ERAI* mouse. However, Venus' stability likely results in the ongoing presence and accumulation of fluorescent protein/signal in situations where ER stress levels have plateaued or are in decline. Based on our findings, we recommend that quantitative measurements of

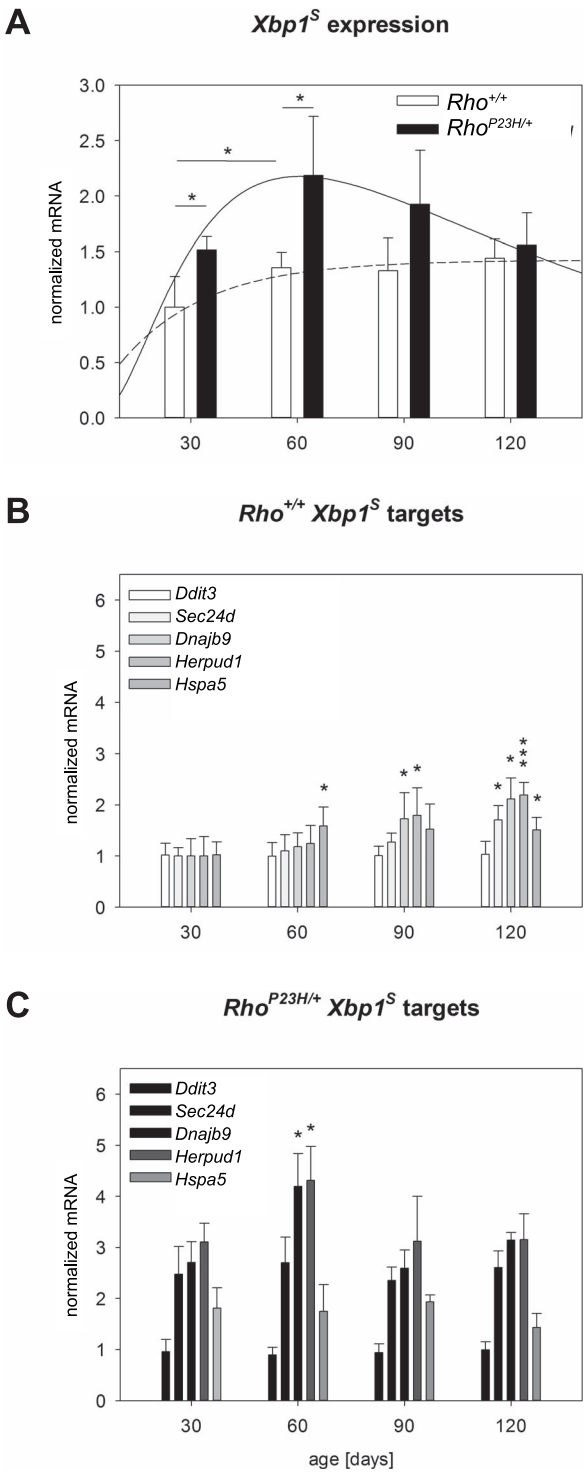

Figure 7. *Xbp1S* mRNA levels and expression levels of XBP1s downstream targets in $Rho^{+/+}$ and $Rho^{P23H/+}$ mouse retinas. $Rho^{P23H/+}$ retinas showed significantly elevated *Xbp1S* transcript levels compared to $Rho^{+/+}$ retinas at ages P30 and P60 (**A**). $Rho^{+/+}$ mice also showed a rather small, but significant, age-dependent increase of *Xbp1S* levels between P30 and P60 in (**A**). Temporal expression of the XBP1 downstream targets *Sec24d*, *Dnajb9*, *Herpud1*, and *Hspa5* followed *Xbp1S* levels in both genotypes (**B**, **C**), while *Ddit3*, a target of the PERK signaling pathway of the UPR, did not show any changes (**B**, **C**). $^{*}P < 0.05$, $^{***}P < 0.001$.

ocular ER stress levels in living *ERAI* mice using fluorescence ophthalmoscopy take into account GFP's half-life and also be accompanied with independent molecular assays for ocular ER stress levels.

Our study is useful in guiding the development of next-generation transgenic mouse GFP reporters of stress. Destabilized GFPs with short half-lives may provide an opportunity to create transgenic mouse stress reporters with fluorescent signals that better reflect dynamic and rapid changes in stress levels.[36] However, stable and strong fluorescent signal also is necessary to visualize the signal in vivo. Finding the right balance between fluorescent signal amplification and dynamic properties will require careful study. Recently, fundus autofluorescence lifetime imaging was performed successfully in eyes of living mice and may provide more sensitive tools to analyze GFP reporters in the eye.[37] In vivo imaging of fluorescence signal from the retinas of GFP reporter mice also may provide a way to rapidly test the clinical efficacy of candidate pharmacologic agents in modulating ER stress levels, especially the growing number of small molecules that target the IRE1 protein.[38–40]

Acknowledgments

During the course of this study, Douglas Yasumura passed away. We are grateful to have worked together with this outstanding scientist for many years over which he became our very close friend.

Supported by VA Merit Award BX002284 (JHL); National Institutes of Health (NIH; Bethesda, MD, USA) Grants EY001919, P30EY002162, and EY006842 (MML); EY020846 and NS088485 (JHL); EY019514 (DBG); and P30EY022589; UCSD Neuroscience Microscopy Shared Facility P30 NS047101; the Foundation Fighting Blindness (MML); Research to Prevent Blindness (DBG); Karl Kirchgessner Foundation (DBG); That Man May See (MVA, DBG); the BrightFocus Foundation (JHL); and postdoctoral support from the Fight-for-Sight Foundation (W-CC). The authors alone are responsible for the content and writing of this paper.

Disclosure: **M.V. Alavi**, None; **W.-C. Chiang**, None; **H. Kroeger**, None; **D. Yasumura**, None; **M.T. Matthes**, None; **T. Iwawaki**, None; **M.M. LaVail**, None; **D.B. Gould**, None; **J.H. Lin**, None

References

1. Alberts B. *Molecular Biology of the Cell*. 5th ed. New York, NY: Garland Science; 2008:1 v. (various pages).
2. Walter P, Ron D. The unfolded protein response: from stress pathway to homeostatic regulation. *Science*. 2011;334:1081–1086.
3. Zhang SX, Sanders E, Fliesler SJ, Wang JJ. Endoplasmic reticulum stress and the unfolded protein responses in retinal degeneration. *Exp Eye Res*. 2014;125:30–40.
4. Zode GS, Sharma AB, Lin X, et al. Ocular-specific ER stress reduction rescues glaucoma in murine glucocorticoid-induced glaucoma. *J Clin Invest*. 2014;124:1956–1965.
5. Zode GS, Kuehn MH, Nishimura DY, et al. Reduction of ER stress via a chemical chaperone prevents disease phenotypes in a mouse model of primary open angle glaucoma. *J Clin Invest*. 2011;121:3542–3553.
6. Kroeger H, LaVail MM, Lin JH. Endoplasmic reticulum stress in vertebrate mutant rhodopsin models of retinal degeneration. *Adv Exp Med Biol*. 2014;801:585–592.
7. Ambati J, Fowler BJ. Mechanisms of age-related macular degeneration. *Neuron*. 2012;75:26–39.
8. Iwawaki T, Akai R, Kohno K, Miura M. A transgenic mouse model for monitoring endoplasmic reticulum stress. *Nat Med*. 2004;10:98–102.

9. Lindsten K, Menendez-Benito V, Masucci MG, Dantuma NP. A transgenic mouse model of the ubiquitin/proteasome system. *Nat Biotech*. 2003;21:897–902.
10. Lobanova ES, Finkelstein S, Skiba NP, Arshavsky VY. Proteasome overload is a common stress factor in multiple forms of inherited retinal degeneration. *Proc Natl Acad Sci U S A*. 2013; 110:9986–9991.
11. Lee AH, Iwakoshi NN, Glimcher LH. XBP-1 regulates a subset of endoplasmic reticulum resident chaperone genes in the unfolded protein response. *Mol Cell Biol*. 2003;23:7448–7459.
12. Shoulders MD, Ryno LM, Genereux JC, et al. Stress-independent activation of XBP1s and/or ATF6 reveals three functionally diverse ER proteostasis environments. *Cell Rep*. 2013;3: 1279–1292.
13. Shimazawa M, Inokuchi Y, Ito Y, et al. Involvement of ER stress in retinal cell death. *Mol Vis*. 2007;13:578–587.
14. Kunte MM, Choudhury S, Manheim JF, et al. ER stress is involved in T17M rhodopsin-induced retinal degeneration. *Invest Ophthalmol Vis Sci*. 2012;53:3792–3800.
15. Chiang WC, Kroeger H, Sakami S, et al. Robust endoplasmic reticulum-associated degradation of rhodopsin precedes retinal degeneration. *Mol Neurobiol*. 2015;52:679–695.
16. Sakami S, Maeda T, Bereta G, et al. Probing mechanisms of photoreceptor degeneration in a new mouse model of the common form of autosomal dominant retinitis pigmentosa due to P23H opsin mutations. *J Biol Chem*. 2011;286:10551–10567.
17. Mattapallil MJ, Wawrousek EF, Chan CC, et al. The Rd8 mutation of the Crb1 gene is present in vendor lines of C57BL/6N mice and embryonic stem cells, and confounds ocular induced mutant phenotypes. *Invest Ophthalmol Vis Sci*. 2012; 53:2921–2927.
18. Mehalow AK, Kameya S, Smith RS, et al. CRB1 is essential for external limiting membrane integrity and photoreceptor morphogenesis in the mammalian retina. *Hum Mol Genet*. 2003;12:2179–2189.
19. Reiling JH, Clish CB, Carette JE, Varadarajan M, Brummelkamp TR, Sabatini DM. A haploid genetic screen identifies the major facilitator domain containing 2A (MFSD2A) transporter as a key mediator in the response to tunicamycin. *Proc Natl Acad Sci U S A*. 2011;108:11756–11765.
20. Fliesler SJ, Rapp LM, Hollyfield JG. Photoreceptor-specific degeneration caused by tunicamycin. *Nature*. 1984;311:575–577.
21. Sohocki MM, Daiger SP, Bowne SJ, et al. Prevalence of mutations causing retinitis pigmentosa and other inherited retinopathies. *Hum Mutat*. 2001;17:42–51.
22. Dryja TP, McGee TL, Reichel E, et al. A point mutation of the rhodopsin gene in one form of retinitis pigmentosa. *Nature*. 1990;343:364–366.
23. Gorbatyuk MS, Knox T, LaVail MM, et al. Restoration of visual function in P23H rhodopsin transgenic rats by gene delivery of BiP/Grp78. *Proc Natl Acad Sci U S A*. 2010;107:5961–5966.
24. Lin JH, Li H, Yasumura D, et al. IRE1 signaling affects cell fate during the unfolded protein response. *Science*. 2007;318:944–949.
25. Chiang WC, Hiramatsu N, Messah C, Kroeger H, Lin JH. Selective activation of ATF6 and PERK endoplasmic reticulum stress signaling pathways prevent mutant rhodopsin accumulation. *Invest Ophthalmol Vis Sci*. 2012;53:7159–7166.
26. Olsson JE, Gordon JW, Pawlyk BS, et al. Transgenic mice with a rhodopsin mutation (Pro23His): a mouse model of autosomal dominant retinitis pigmentosa. *Neuron*. 1992;9:815–830.
27. Harding HP, Novoa I, Zhang Y, et al. Regulated translation initiation controls stress-induced gene expression in mammalian cells. *Mol Cell*. 2000;6:1099–1108.
28. Oikawa D, Akai R, Tokuda M, Iwawaki T. A transgenic mouse model for monitoring oxidative stress. *Sci Rep*. 2012;2:229.
29. Bennett J, Duan D, Engelhardt JF, Maguire AM. Real-time, noninvasive in vivo assessment of adeno-associated virus-mediated retinal transduction. *Invest Ophthalmol Vis Sci*. 1997;38:2857–2863.
30. Delori F, Greenberg JP, Woods RL, et al. Quantitative measurements of autofluorescence with the scanning laser ophthalmoscope. *Invest Ophthalmol Vis Sci*. 2011;52:9379–9390.
31. Henis-Korenblit S, Zhang P, Hansen M, et al. Insulin/IGF-1 signaling mutants reprogram ER stress response regulators to promote longevity. *Proc Natl Acad Sci U S A*. 2010;107:9730–9735.
32. Taylor RC, Dillin A. XBP-1 is a cell-nonautonomous regulator of stress resistance and longevity. *Cell*. 2013;153:1435–1447.
33. Nagai T, Ibata K, Park ES, Kubota M, Mikoshiba K, Miyawaki A. A variant of yellow fluorescent protein with fast and efficient maturation for cell-biological applications. *Nat Biotechnol*. 2002;20:87–90.
34. Corish P, Tyler-Smith C. Attenuation of green fluorescent protein half-life in mammalian cells. *Protein Eng*. 1999;12: 1035–1040.
35. Calfon M, Zeng H, Urano F, et al. IRE1 couples endoplasmic reticulum load to secretory capacity by processing the XBP-1 mRNA. *Nature*. 2002;415:92–96.
36. Dantuma NP, Lindsten K, Glas R, Jellne M, Masucci MG. Short-lived green fluorescent proteins for quantifying ubiquitin/proteasome-dependent proteolysis in living cells. *Nat Biotechnol*. 2000;18:538–543.
37. Dysli C, Dysli M, Enzmann V, Wolf S, Zinkernagel MS. Fluorescence lifetime imaging of the ocular fundus in mice. *Invest Ophthalmol Vis Sci*. 2014;55:7206–7215.
38. Ghosh R, Wang L, Wang ES, et al. Allosteric inhibition of the IRE1α RNase preserves cell viability and function during endoplasmic reticulum stress. *Cell*. 2014;158:534–548.
39. Papandreou I, Denko NC, Olson M, et al. Identification of an Ire1alpha endonuclease specific inhibitor with cytotoxic activity against human multiple myeloma. *Blood*. 2011;117: 1311–1314.
40. Cross BC, Bond PJ, Sadowski PG, et al. The molecular basis for selective inhibition of unconventional mRNA splicing by an IRE1-binding small molecule. *Proc Natl Acad Sci U S A*. 2012; 109:E869–E878.

Investigative Ophthalmology & Visual Science

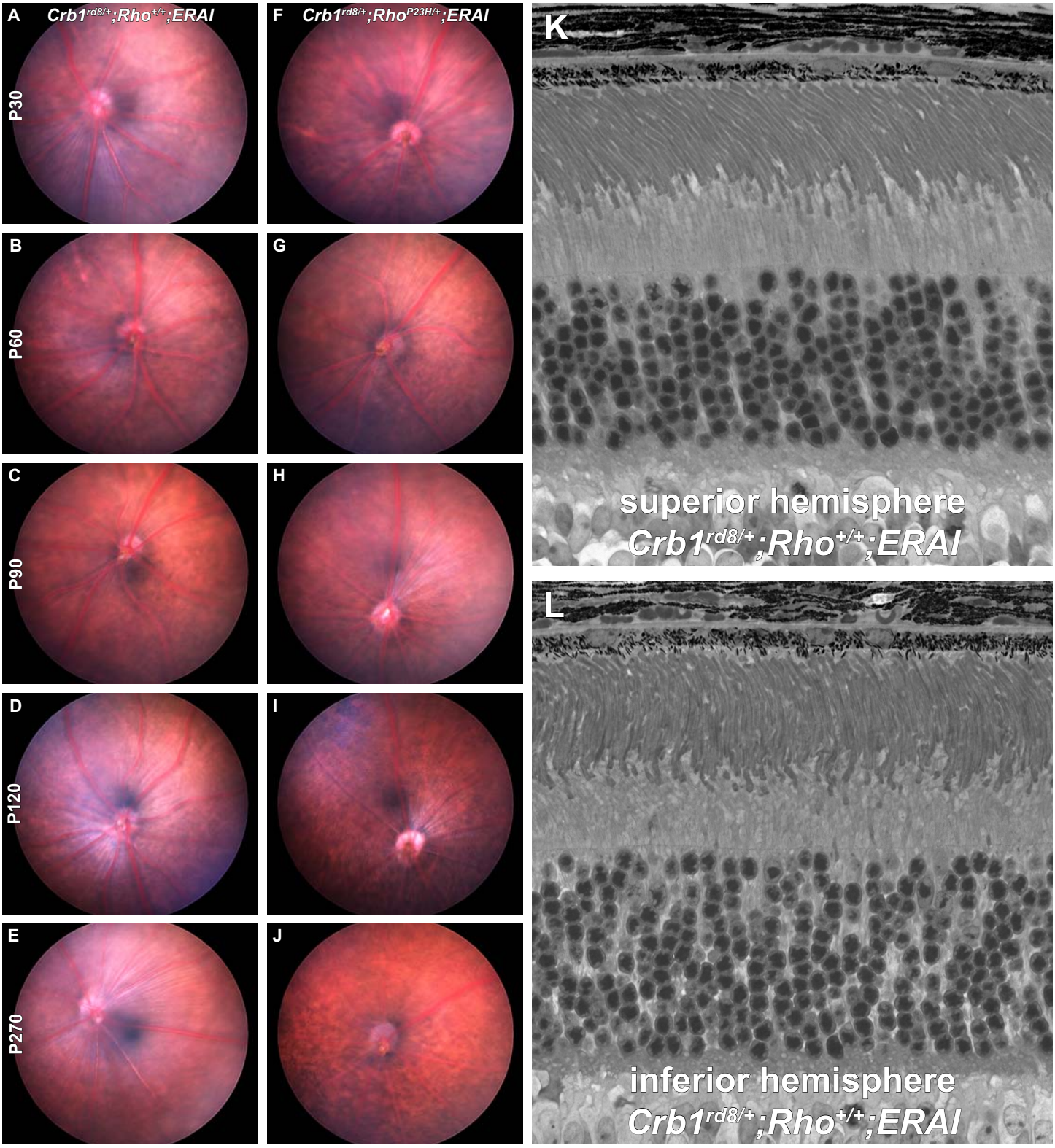

supplemental Figure 1

Supplemental Figure 1: Unremarkable fundus of *Rho$^{+/+}$;ERAI* mice and *Rho$^{P23H/+}$;ERAI* mice.

Fundus of *Rho$^{+/+}$;ERAI* mice (A-E) and *Rho$^{P23H/+}$;ERAI* mice (F-J) at the investigated ages presented without pathological findings. The morphology of two P120 *Rho$^{+/+}$;ERAI* mice was also unremarkable (K and L).